

Interplay of Higgs and Sparticle Masses in the CMSSM with updated SUSY constraints

Alexander Belyaev^a, Shahida Dar^b, Ilia Gogoladze^b, Azar Mustafayev^c and Qaisar Shafi^b

^a*School of Physics and Astronomy, University of Southampton, Highfield, Southampton SO17 1BJ, UK; E-mail: a.belyaev@phys.soton.ac.uk*

^b*Bartol Research Institute, Department of Physics & Astronomy, University of Delaware, Newark, DE 19716, USA;*

E-mail: dars@physics.udel.edu, ilia@physics.udel.edu, shafi@bartol.udel.edu

^c*Department of Physics and Astronomy, University of Kansas, Lawrence, KS 66045, USA; E-mail: amustaf@ku.edu*

ABSTRACT: We estimate the bounds on Higgs and sparticle masses and discuss their correlations in the constrained minimal supersymmetric standard model (CMSSM). In our analysis we have applied the present constraints from collider and low energy experiments, as well as the experimental bound on cold dark matter from WMAP. For a given lightest Higgs boson mass, which is expected to be measured with good precision at the LHC, we find important correlations between the Higgs and sparticle masses which allows one to delineate the MSSM model parameters and particle spectra. We have also demonstrated an important complementarity between the LHC and direct dark matter detection experiments emphasizing that by including the experimental input both from collider physics and from dark matter detection experiments, one would significantly improve the measurement of the SUSY spectrum and the underlying parameter space.

KEYWORDS: Supersymmetry Phenomenology, Supergravity Models, Supersymmetric Standard Model, CMSSM, Dark Matter.

1. Introduction

In recent years the measured value of the top quark mass has gradually inched its way down to its current value of 170.9 ± 1.8 GeV [1], which is significantly below the central value of around 178 GeV used in various studies just a few years ago. This downward shift of the top quark mass has important implications for the particle spectrum of the minimal supersymmetric standard model (MSSM), in particular for the lightest CP-even Higgs boson mass, m_h , since the leading radiative corrections to m_h are proportional to the square of the top mass, m_t^2 , while $m_h \geq 114.4$ GeV from LEP2 in the decoupling limit [2]. At tree level $m_h \leq M_Z |\cos 2\beta|$, and so significant radiative corrections are necessary to overcome the LEP2 bound. In the absence of large trilinear couplings, significant radiative corrections can be generated only if the stop masses are in the TeV range. Alternatively, significant stop mixing in the presence of large trilinear couplings can drive m_h up without excessively heavy stops. In this paper, we investigate both possibilities and study the correlations of the Higgs and sparticle mass spectrum in the constrained MSSM (CMSSM) [3, 4, 5, 6, 7] under the plausible assumption that the neutralino constitutes the cold dark matter in the universe.

The CMSSM has received a great deal of attention in recent years, especially for m_t close to 178 GeV [8, 9, 10, 11, 12, 13, 14, 15, 16, 17, 18]. When we started this analysis, the central value was $m_t = 171.4 \pm 2.1$ GeV [19], which has recently drifted slightly lower to 170.9 ± 1.8 GeV [1]. Our results are based on $m_t = 171.4$ GeV. Note that we have found agreement between our results with partially overlapping results of some recent papers which also use an updated value for the top-quark mass [20, 21, 22, 23].

The CMSSM contains the following five fundamental parameters (we follow notations and conventions of Ref. [24])

$$m_0, m_{1/2}, A_0, \tan \beta, \text{sign}(\mu), \quad (1.1)$$

where m_0 is the universal soft supersymmetry breaking (SSB) scalar mass, $m_{1/2}$ the universal SSB gaugino mass, and A_0 the universal SSB trilinear scalar interaction (with the corresponding Yukawa coupling factored out). The values for these three parameters are prescribed at the GUT scale, $M_{GUT} \simeq 2 \times 10^{16}$ GeV. $\tan \beta$ is the ratio of the vacuum expectation values (VEV) of the two Higgs doublets at the weak scale, and μ is the supersymmetric bilinear Higgs parameter whose magnitude, but not the sign, is determined by the radiative electroweak breaking conditions¹.

The results for CMSSM studies are usually presented in the $(m_0, m_{1/2})$ plane. However, anticipating that the lightest MSSM Higgs will be found at the LHC and that its mass according to ATLAS [28] and CMS [29] technical design reports, will be determined to a precision which is better than 1%, it is worthwhile to understand possible correlations

¹Historically this framework is also called mSUGRA and is associated with supergravity. However, supergravity does not necessarily lead to high scale universality as originally thought. Occasionally, the abbreviation mSUGRA is used only for a subset of (1.1) where some additional relations coming from a particular form of Kähler potential are assumed (see e.g. [25, 26]). To avoid possible confusion, we decided to use the term CMSSM and refer interested readers to Ref. [24, 27] for textbook discussions.

between such a precisely measured Higgs mass and sparticles masses as well as the underlying model parameters. Such correlations would allow one to delineate the underlying SUSY model and, moreover, to predict some model parameters and masses, such as the trilinear coupling, A_t , whose measurement at the LHC may be problematic. The mass m_h may be experimentally determined to an accuracy better than a GeV, which is better than the theoretical calculation of m_h at present [30]. In this study, we assumed a theoretical uncertainty Δm_h of 1 GeV in estimating the precision with which the sparticles masses and model parameters are predicted as a function of m_h , keeping in mind the optimistic hope that the theoretical uncertainty for the Higgs mass calculation will be improved by the time of the actual Higgs boson search at the LHC. In our analysis we require that the magnitudes of $m_{1/2}$ and A_0 should not exceed 2 TeV, while m_0 is taken to be $\lesssim 5$ TeV. This choice covers the whole dark matter-motivated CMSSM parameter space except the focus point region (see discussion below), which can go with m_0 all the way up to M_{GUT} , and turning the CMSSM scenario into a split-SUSY one [31].

The sign of the MSSM parameter μ is taken to be positive, as dictated by the experimental measurements of the anomalous magnetic moment of the muon, Δa_μ . We take into account the LEP2 constraints on the chargino mass, experimental data on rare B decays, and the WMAP relic density constraints.

The paper is organized as follows. In Section 2 we review details of the MSSM parameter space scan and implementation of the various constraints. In Section 3 we present our results on various correlations of the MSSM spectra which would be crucial for LHC collider phenomenology, and in Section 4 we summarize our conclusions.

2. SUSY constraints and scanning procedure

For the MSSM spectrum calculation we use the IsaSUGRA program, which is a part of ISAJET 7.74 package [32]. In this package, the weak scale values of gauge and third generation Yukawa couplings are evolved to M_{GUT} via the MSSM renormalization group equations (RGEs) in the \overline{DR} regularization scheme, where M_{GUT} is defined to be the scale at which $g_1 = g_2$. We do not enforce an exact unification of the strong coupling $g_3 = g_1 = g_2$ at M_{GUT} , since a few percent deviation from unification can be assigned to unknown GUT-scale threshold corrections [33, 34]. At M_{GUT} , the universal soft supersymmetry breaking (SSB) boundary conditions are imposed and all SSB parameters along with the gauge and Yukawa couplings are evolved back to the weak scale M_Z . In the evaluation of Yukawa couplings the SUSY threshold corrections [35] are taken into account at the common scale $M_{SUSY} = \sqrt{m_{\tilde{t}_L} m_{\tilde{t}_R}}$, and the entire parameter set is iteratively run between M_Z and M_{GUT} using full 2-loop RGEs until a stable solution is obtained. To better account for leading-log corrections, one-loop step-beta functions are adopted for gauge and Yukawa couplings and the SSB parameters m_i are extracted from RGEs at multiple scales $m_i = m_i(m_i)$.² The RGE-improved 1-loop effective potential is minimized at an optimized scale M_{SUSY} , which effectively accounts for the leading 2-loop corrections. Full 1-loop radiative corrections are

²Detailed discussion of SUSY threshold effects in ISAJET and other public codes can be found in ref. [36].

incorporated for all sparticle masses according to ref. [35]. The numerical results are in close accord with those generated by the FeynHiggsFast program [37].

The requirement of radiative electroweak symmetry breaking (REWSB) [38, 39, 40, 41] puts an important theoretical constraint on the parameter space. Another important constraint comes from limits on the cosmological abundance of stable charged particles [42] – this excludes the parameter points where charged SUSY particles, such as $\tilde{\tau}_1$ or \tilde{t}_1 , become the lightest supersymmetric particle (LSP).

We also impose bounds on sparticle masses resulting from direct searches at colliders. The LEP2 search for pair production of sleptons [43] puts the lower limit $m_{\tilde{l}} \geq 99$ GeV provided the mass difference $m_{\tilde{l}} - m_{\tilde{Z}_1} > 10$ GeV. Another important LEP2 constraint comes from the lightest chargino [44], $m_{\tilde{W}_1} \geq 103.5$ GeV.

Recent search results for squark/gluino production at the Tevatron [45, 46] put bounds on the gluino mass $m_{\tilde{g}} > 370$ GeV for $m_{\tilde{q}} \simeq m_{\tilde{g}}$, and $m_{\tilde{g}} > 220$ GeV for $m_{\tilde{q}} < m_{\tilde{g}}$. In models with gaugino mass universality, like CMSSM, $m_{\tilde{g}} \sim 3.5m_{\tilde{W}_1}$. Thus, the LEP2 chargino bound translates into a bound on the gluino mass, $m_{\tilde{g}} \geq 350$ GeV, to which Tevatron comes close only for $m_{\tilde{q}} \simeq m_{\tilde{g}}$.

Tevatron searches for direct pair production of stops [47, 48] impose the bound $m_{\tilde{t}_1} > 132$ GeV for $m_{\tilde{Z}_1} \leq 48$ GeV. However, the requirements of GUT-scale gaugino mass universality tell us that $m_{\tilde{Z}_1} \simeq 0.5m_{\tilde{W}_1} \geq 51$ GeV for points satisfying the LEP2 chargino bound. This chargino-neutralino mass ratio gets smaller in the HB/FP region at large m_0 , but here the stops are always heavier than about 500 GeV, as we will show later.

Similar searches for direct pair production by D0 collaboration [49] put a bound $m_{\tilde{b}_1} > 222$ GeV for $m_{\tilde{Z}_1} \leq 90$ GeV; the CDF limit is slightly lower, $m_{\tilde{b}_1} > 193$ GeV for $m_{\tilde{Z}_1} \leq 80$ GeV [47]. In CMSSM, the lightest sbottom is dominantly left-handed whose mass is given by the approximate relation $m_{\tilde{b}_L}^2 \sim 0.52m_0^2 + 5m_{1/2}^2$. The lightest chargino is mostly wino and obeys the approximate relation $m_{\tilde{W}_1} \sim \frac{2}{3}m_{1/2}$. Therefore, the LEP2 chargino bound leads to $m_{\tilde{b}_L} > 350$ GeV, significantly above the Tevatron limit.

The LEP2 Higgs bound [2] further constrains the MSSM parameter space. After the LEP2 direct SUSY searches constraints are applied, the pseudoscalar mass m_A is limited to be above 200 GeV (as we present later on), which ensures the decoupling regime and SM-like coupling of h to gauge bosons. Therefore, the SM-Higgs LEP2 bound $m_h \geq 114.4$ GeV is applicable to the CMSSM scenario. This bound can be very different in the MSSM light Higgs boson scenario [50], when the LEP2 bound allows a higgs scalar as light as about 60 GeV. We would like to point out that in our plots we do not remove points with the Higgs boson mass below the SM-higgs LEP2 bound, but indicate its position whenever possible for the sake of clarity.

A combination of the recent WMAP data with other cosmological observations leads to tight constraints on the cold dark matter (CDM) relic abundance, and the most important and dramatic constraint on the CMSSM parameter space. The exact numerical value depends on a number of assumptions about the history of the early Universe [51] as well as on a combination of data sets chosen. In our analysis we use the constraints arising from

a combination of WMAP and the Sloan Digital Sky Survey data [52]

$$\Omega_{\text{CDM}}h^2 = 0.111^{+0.011}_{-0.015} \quad (2\sigma), \quad (2.1)$$

which assumes standard Λ CDM cosmology. We further assume that the bulk of CDM is composed of the lightest neutralino \tilde{Z}_1 which was in thermal equilibrium in the early Universe³. To evaluate the neutralino relic density we employed the IsaReD code [54] (part of IsaTools package), which uses several thousands $2 \rightarrow 2$ annihilation and co-annihilation Feynman diagrams generated by the CompHEP package [55, 56].

An important constraint comes from the measurement of the muon anomalous magnetic moment $a_\mu = \frac{(g-2)_\mu}{2}$ by the E821 collaboration [57]. The current experimental value, $a_\mu^{\text{exp}} = (11659208.0 \pm 6.3) \times 10^{-10}$ deviates by 3.4σ from the SM prediction which uses hadronic vacuum polarization determined from e^+e^- annihilation data, but there is no significant deviation from the SM predictions if the hadronic contribution is calculated using τ -decay data [58, 59, 60]. There is a stronger and stronger tendency at present to prefer e^+e^- data to evaluate the lowest-order hadronic contribution to a_μ . The most recent analysis performed in ref. [58], based on e^+e^- data, yields a deviation $\Delta a_\mu = (27.5 \pm 8.4) \times 10^{-10}$ from the experimental value. In view of the lack of consensus on the computation of the SM part [58, 59, 60], we have decided not to apply the $(g-2)_\mu$ constraint but to indicate the 3σ allowed region for $(g-2)_\mu$,

$$3.4 \times 10^{-10} \leq \Delta a_\mu \leq 55.6 \times 10^{-10}, \quad (2.2)$$

with special colors to allow readers to make their own judgment on this constraint. This 3σ interval uses $(g-2)_\mu$ predictions based on e^+e^- data and was taken from the latest summary of $(g-2)_\mu$ status [61].

We used IsaAMU subroutine described in ref. [62] to evaluate the SUSY contribution to $(g-2)_\mu$. The contribution of SUSY particles comes from $\widetilde{W}_i \tilde{\nu}_\mu$ and $\tilde{Z}_i \tilde{\mu}_{1,2}$ loops, where the total chargino contributions dominates in CMSSM. Therefore, $(g-2)_\mu$ puts an upper limit on the masses of charginos, neutralinos and second generation sleptons. For $\tan\beta$ not too small, $\Delta a_\mu^{\text{SUSY}} \propto \mu M_2 \tan\beta / \tilde{m}^4$, where M_2 is the $SU(2)$ gaugino mass and \tilde{m} is the heaviest mass in the loop. Thus, it is particularly important for large $\tan\beta$ values and light sleptons and -inos (*i.e.*, small m_0 and $m_{1/2}$ region). Note also that for models with a positive gaugino mass, like CMSSM, the sign of μ has to be positive.

The good agreement of the experimental value of the flavor changing $b \rightarrow s\gamma$ decay rate with the SM result imposes an important constraint on any beyond the SM physics. In MSSM, the most important SUSY contributions come from tH^\pm and $\tilde{t}\widetilde{W}^\pm$ loops. To evaluate the SM+MSSM branching fraction, we employed the IsaBSG subroutine [63, 64], which uses the effective theory approach. Namely, when any sparticle threshold is crossed, the sparticle is integrated out, thereby inducing a new effective-operator basis. The resulting Wilson coefficients are evolved down to $Q = m_b$, thus summing large logarithms that can occur from the disparity between the scales at which various particles enter the loop corrections. In the CMSSM, the assumed universality of soft SUSY breaking (SSB)

³Non-thermalized neutralinos were recently discussed in ref. [53]

masses leads to a particularly simple framework known as minimal flavor violation (MFV) in which flavor mixing arises only from the CKM matrix. The experimental world average measurement for $Br(b \rightarrow s\gamma)$ is known to be $(3.55 \pm 0.26) \times 10^{-4}$ [65], while its updated SM prediction has been recently shifted down to $(3.15 \pm 0.23) \times 10^{-4}$ value [66, 67]. Combining the experimental and theoretical errors in quadratures we apply the following constraints at 2σ level in our study:

$$2.85 \times 10^{-4} \leq Br(b \rightarrow s\gamma) \leq 4.24 \times 10^{-4}. \quad (2.3)$$

This conservative approach has two advantages. Firstly, it allows one to accommodate the theoretical uncertainties that mainly come from the residual scale dependence and are $\sim 12\%$ [68]. Secondly, the SSB terms might have small off-diagonal entries at M_{GUT} that will change $Br(b \rightarrow s\gamma)$ without significantly affecting other quantities.

Another B-physics constraint comes from the upper limit on $B_s \rightarrow \mu^+ \mu^-$ decay branching fraction,

$$BF(B_s \rightarrow \mu^+ \mu^-) < 1.0 \times 10^{-7}, \quad (2.4)$$

as was reported by the CDF collaboration [69]. We compute the SUSY contribution using IsaBMU code [70] which assumes MFV. The SM predicts a very small value for this branching fraction, namely $BF_{SM}(B_s \rightarrow \mu^+ \mu^-) \simeq 3.4 \times 10^{-9}$, while the SUSY contribution behaves as $\tan^6 \beta / m_A^4$ and hence is particularly important at large $\tan \beta$. However, it turns out that this constraint is always superseded in the CMSSM parameter space under study by the one from $b \rightarrow s\gamma$.

To find bounds and correlations for the Higgs and sparticle masses, we performed random scans for the following range of the CMSSM parameters:

$$\begin{aligned} 0 \leq m_0 \leq 5 \text{ TeV}, & \quad 0 \leq m_{1/2} \leq 2 \text{ TeV} \\ A_0 = 0.5 \text{ TeV}, 0, -1 \text{ TeV}, -2 \text{ TeV}, & \quad \tan \beta = 5, 10, 50 \text{ and } 53 \end{aligned} \quad (2.5)$$

with $\mu > 0$ and $m_t = 171.4 \text{ GeV}$. We have also performed scans for intermediate values of $\tan \beta = 30, 45$, but found results to be similar to $\tan \beta = 10, 50$ cases respectively and decided to omit them. The use of IsaTools package for implementation of the various constraints mentioned above was crucial in our study.

3. Results

Let us first demonstrate our procedure by consecutively applying the constraints mentioned in the previous section to the case with $A_0 = -2 \text{ TeV}$ and $\tan \beta = 10$. We start by presenting our results in the conventional $(m_0, m_{1/2})$ plane illustrated in Fig. 1. Frame a) displays the colored points allowed by radiative electroweak symmetry breaking (REWSB) and from the requirement that the neutralino is the LSP ⁴.

⁴In fact, to keep the data set size manageable, we show only points where $\Omega h^2 \leq 10$. The CMSSM points with too high a relic density, denoted by gray or white color above the gray-colored area, are not relevant to the current discussion.

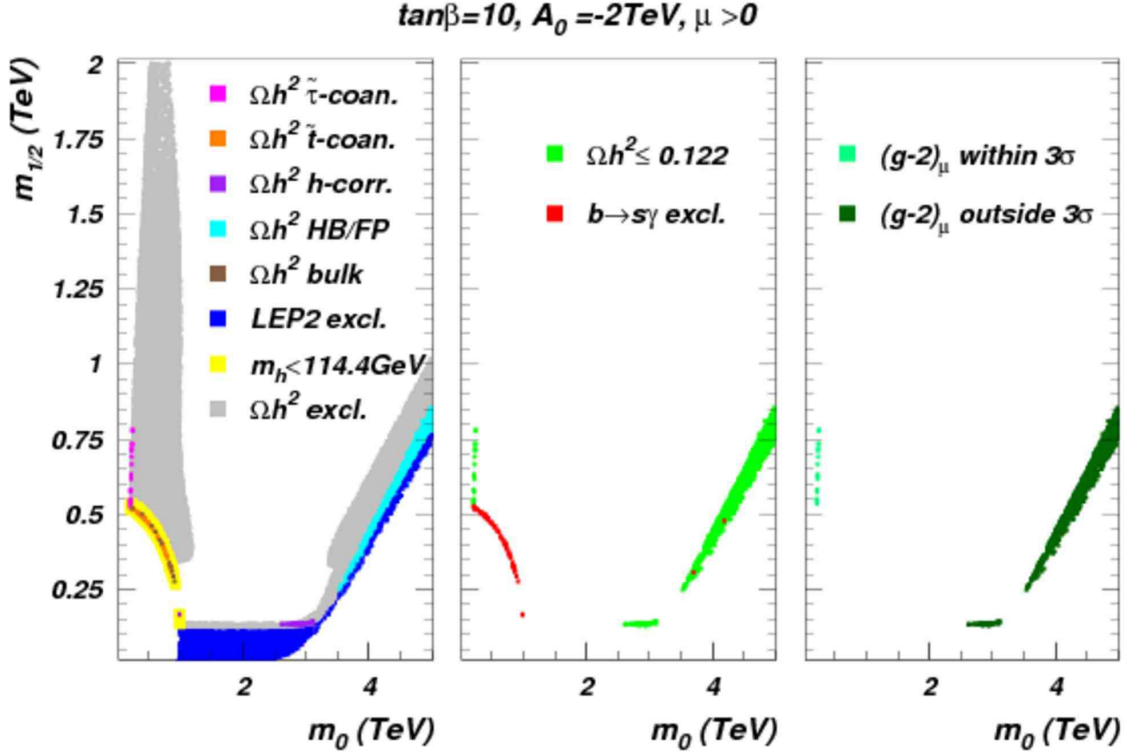


Figure 1: $(m_0, m_{1/2})$ plane for $\tan\beta = 10$, $A_0 = -2$ TeV. In frame a), the gray regions are excluded by WMAP, blue ones are excluded by LEP2 chargino bound, and the yellow region has m_h below 114.4 GeV; the remaining colors denote various WMAP-allowed regions described in the text. In frame b), the green regions satisfy both the WMAP and $b \rightarrow s\gamma$ constraints, while the red region satisfies the WMAP bound but fails the $b \rightarrow s\gamma$ constraint. In frame c), regions surviving the WMAP and $b \rightarrow s\gamma$ constraint are presented; light (dark) green region corresponds to $(g-2)_\mu$ within (outside) the 3σ range (2.2).

The gray region at low m_0 and large-to-medium $m_{1/2}$ values at the left is excluded because $m_{\tilde{\tau}_1} < m_{\tilde{Z}_1}$, while the white bulge at low m_0 and low $m_{1/2}$ under the \tilde{t} -coannihilation contour is excluded because the top-squark is LSP in this region (typical for such a large negative A_0). Finally, the white corner region at the bottom-right below the colored band is excluded because of the failure of the REWSB condition. The LEP2 constraint on chargino mass removes the points shown in blue color. After application of the WMAP upper bound on LSP DM, the allowed region is drastically shrunk to several small regions of the parameter space, with the remaining gray points associated with unacceptably high DM relic density. This exhibits a well known fact that in CMSSM the neutralinos do not efficiently annihilate in the early universe except in a few very special narrow regions of the parameter space⁵:

- the bulk region at low m_0 and low $m_{1/2}$, shown in brown color, where neutralinos efficiently annihilate via t -channel slepton exchange. This area is almost completely ruled out by LEP2 searches [71, 72, 73, 74].

⁵These regions sometimes appear discontinuous on some plots only due to the finite resolution of our scan.

- the stau co-annihilation region ($\tilde{\tau}\tilde{Z}$) [75, 76, 77, 78, 79, 80, 81, 82, 54] at low m_0 , shown in magenta color, where $m_{\tilde{Z}_1} \simeq m_{\tilde{\tau}_1}$ and rapid reactions $\tilde{Z}_1\tilde{\tau}_1 \rightarrow X$ and $\tilde{\tau}_1\tilde{\tau}_1 \rightarrow X$ (here X stands for any allowed final state of SM and/or higgs particles) in the early universe lower the neutralino relic density to the WMAP range (2.1);
- the stop coannihilation region ($\tilde{t}\tilde{Z}$) appearing at low m_0 and low $m_{1/2}$, but for particular values of A_0 , shown in orange color, where $m_{\tilde{Z}_1} \simeq m_{\tilde{t}_1}$ [83, 84, 85];
- the hyperbolic branch/focus point region (HB/FP) at large m_0 , shown in turquoise, where $|\mu|$ is small and the neutralino develops a substantial higgsino component that enhances its annihilation into WW , ZZ and Zh pairs in the early universe [86, 87, 88, 89, 90];
- the h -corridor (HF) at low $m_{1/2}$, shown in purple color, where $2m_{\tilde{Z}_1} \simeq m_h$ and efficient annihilation through the light MSSM Higgs boson resonance occurs in the early universe [91, 73];
- the A -annihilation funnel (AF) that appears only at suitably large values of $\tan\beta$ and is therefore absent in the current plot. In this case, $2m_{\tilde{Z}_1} \simeq m_A$ and resonance annihilation of neutralinos via the broad A and H Higgs bosons becomes possible [92, 93, 94, 95, 96, 97].

Next, in frame b), we show the effect of the $b \rightarrow s\gamma$ constraint on the WMAP allowed region: red points denote the excluded region where the branching fraction exceeds the range (2.3) which covers the bulk region, stop coannihilation and the low $m_{1/2}$ part of the stau coannihilation regions. The green points survive the combination of the WMAP and $b \rightarrow s\gamma$ and are the subject of our analysis in this paper. Finally, in frame c) we illustrate the effect of $(g-2)_\mu$ constraint (2.2) which, at 3σ level, excludes the h -corridor and HB/FP regions at medium and high m_0 , denoted by dark green color. This occurs since sleptons are heavy in these regions and their loop contributions do not make significant contributions to $(g-2)_\mu$. On the contrary, in the $\tilde{\tau}\tilde{Z}$ region, shown in light green color, the sleptons are light and can account for the observed deviation (2.2).

In Fig. 2 we present results for the same parameter space, but in the (m_h, m_A) plane with the color coding as in Fig. 1. Note that the LEP2 Higgs boson limit excludes the $\tilde{t}\tilde{Z}$ region, leaving $\tilde{\tau}\tilde{Z}$, HF and HB/FP regions respecting the WMAP dark matter constraint. It is very noticeable, that the regions allowed by SUSY constraints appear as very narrow bands exhibiting an obvious correlation of m_A with m_h . This correlation is related to the two-fold solutions mainly defined by the DM constraints: the lower band corresponding to $\tilde{\tau}\tilde{Z}$ region (connected to $\tilde{t}\tilde{Z}$ and AF regions at high values of $\tan\beta$) and the upper band corresponding to the HB/FP region (and connected to HF region at low to intermediate values of $\tan\beta$).

Qualitatively similar patterns can be observed for other A_0 and $\tan\beta$ values and are presented in Fig. 3. Here gray, light green, light blue, and orange colors correspond to $\tan\beta = 5, 10, 50$ and 53 respectively and satisfy the 3σ bound on Δa_μ given by Eq.(2.2). Black, dark green, blue and red colors correspond to the region outside the Δa_μ 3σ bound;

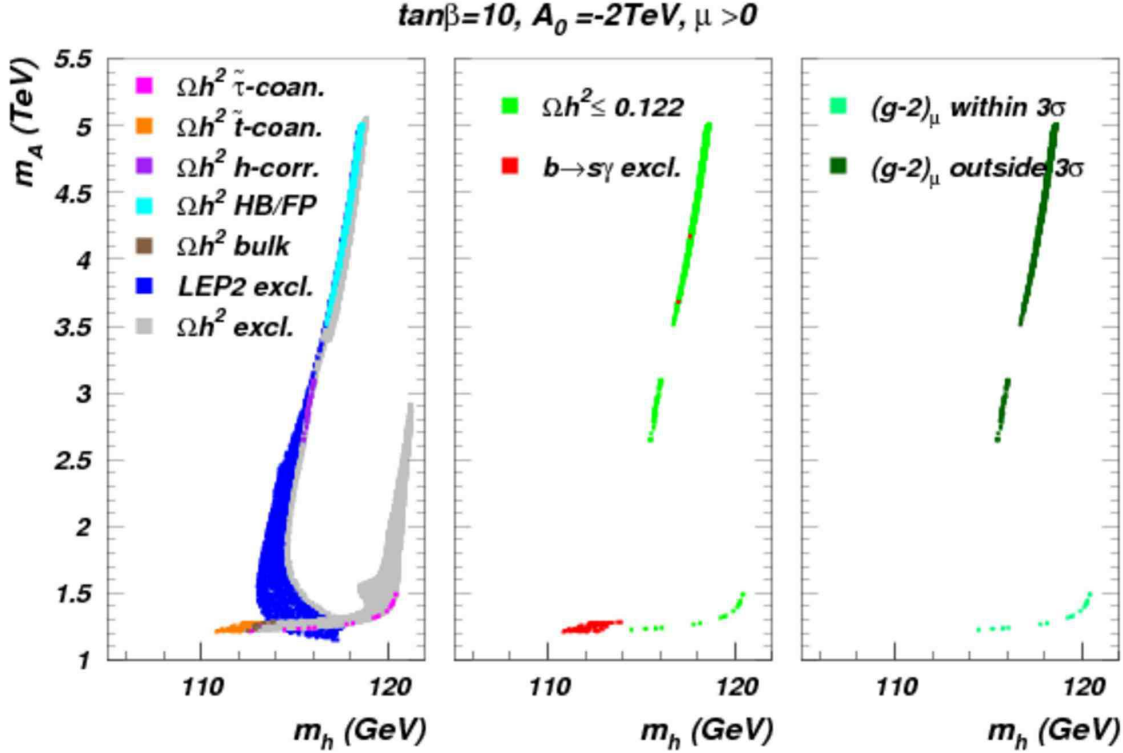


Figure 2: (m_h, m_A) plane for $\tan\beta = 10$, $A_0 = -2$ TeV. The color code is the same as in Fig. 1.

frames a), b), c), d) present results for $A_0 = 0.5, 0, -1$ and -2 TeV respectively. The upper and lower bands for each color represent the HB/FP(+HF) and $\tilde{\tau}\tilde{Z}$ (+ $\tilde{t}\tilde{Z}$ +AF) regions respectively. One finds that the CP-odd Higgs boson mass is always above ~ 200 GeV, corresponding to the decoupling regime and SM-like nature of h . One can see that for $A_0 = 0.5$ TeV and 0 (frames a) and b) respectively) the parameter space for $\tan\beta = 5$ is completely excluded by the LEP2 limit, $m_h \geq 114.4$ GeV. This is due to the low tree-level Higgs mass and the absence of large enough radiative corrections. However, for $A_0 = -1$ TeV and -2 TeV (frames c) and d) respectively), enhanced radiative corrections to the Higgs boson mass open up some viable CMSSM parameter space even for $\tan\beta$ as low as 5 . We note here that at the EW scale m_h depends, to a good approximation [98], on the absolute value of A_0 . Starting with negative values of A_t at M_{GUT} , it turns out that A_t evolves to even larger negative values at the EW scale, thereby enhancing m_h and relaxing the lower bounds on the masses of the SUSY particles. This explains our choice for A_0 values used in the paper.

We stress that the light colors in Fig. 3 and subsequent figures represent the parameter space which respect all of the constraints mentioned above *including* $(g-2)_\mu$, while the dark colors represent the parameter space respecting all constraints *except* $(g-2)_\mu$. For low and intermediate values of $\tan\beta$ only some portion of the $\tilde{\tau}$ -coannihilation regions (lower curves) denoted by gray ($\tan\beta = 5$) and light green ($\tan\beta = 10$) colors satisfy all of the constraints, while the focus point region is excluded. In fact, this known feature of CMSSM represents the tension between essentially two constraints: $b \rightarrow s\gamma$ and $(g-2)_\mu$. The root

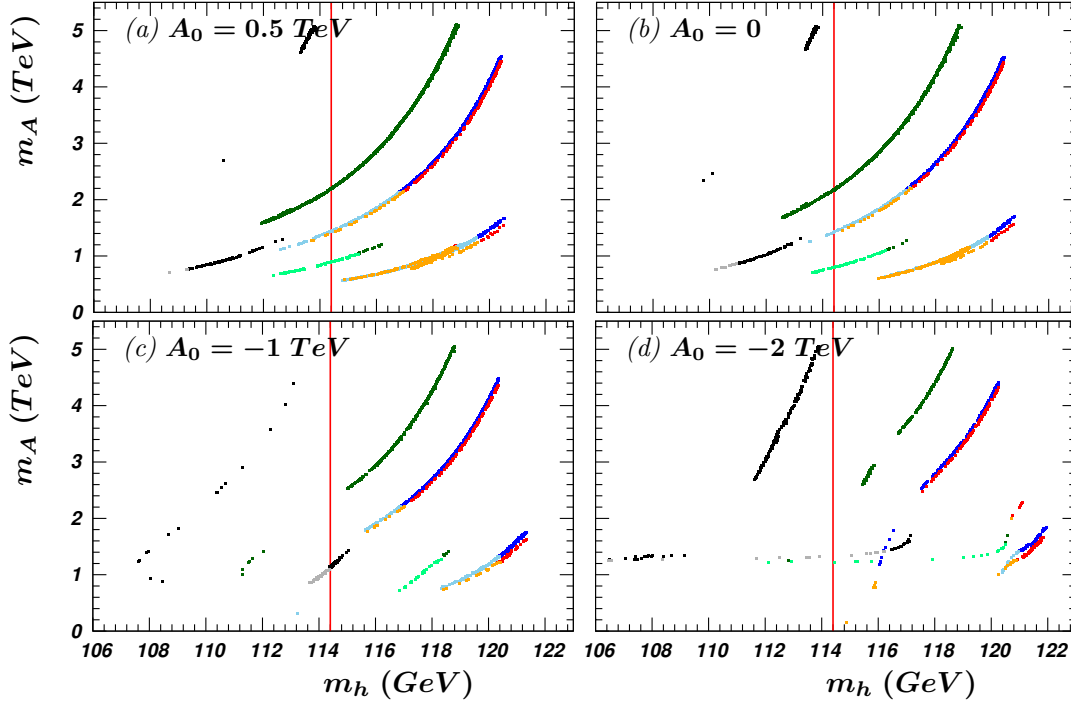


Figure 3: Allowed region for CP-odd Higgs boson mass m_A versus m_h . Gray, light green, light blue, and orange correspond to $\tan \beta = 5, 10, 50$ and 53 respectively and satisfy the 3σ bound on Δa_μ (2.2). Black, dark green, blue and red correspond to $\tan \beta = 5, 10, 50$ and 53 , with Δa_μ outside the 3σ range.

cause of this tension is the universality condition in CMSSM which implies equal squark and slepton soft mass parameters at M_{GUT} . On the other hand, $b \rightarrow s\gamma$ data agrees with the SM prediction (implying *heavy* third generation of squarks at the EW scale) whereas there seems to be quite a significant deviation between the SM prediction and $(g - 2)_\mu$ measurement (implying *light* second generation of sleptons at the EW scale). It has been shown [15] that this tension can be resolved either with large $\tan \beta$ values or, alternatively, by relaxing the GUT-scale generation universality condition. Indeed, one can see that at large $\tan \beta$ there are allowed regions with both upper and lower (light blue ($\tan \beta = 50$) and orange ($\tan \beta = 53$)) curves. In the case of large $\tan \beta$, m_A (m_H) up to about 1 TeV can be accessible at the LHC and used for a consistency check of the CMSSM.

In Fig. 4 we present correlations between the gluino and the light Higgs boson masses with the same color coding as in the previous figure. The pattern of bands in the $(m_{\tilde{g}}, m_h)$ plane is quite different from the one for (m_A, m_h) in the previous figure. Gluino mass is mainly defined by $m_{1/2}$ which, in turn, is similarly correlated with m_h along the $\tilde{\tau}\tilde{Z}$ and HB/FP regions. In the $(m_{\tilde{g}}, m_h)$ plane the bands are close to each other. The gluino mass increases in the ‘far’ HB/FP region of large m_0 and large $m_{1/2}$, since in this region $m_{1/2}$ goes beyond 1 TeV where the $\tilde{\tau}\tilde{Z}$ region typically ends. The ‘far’ HB/FP region is characterized by the heaviest m_h and heaviest gluino mass in this particular plane. Notice that the gluino mass is always above 400-500 GeV, so that the recent Tevatron bounds on

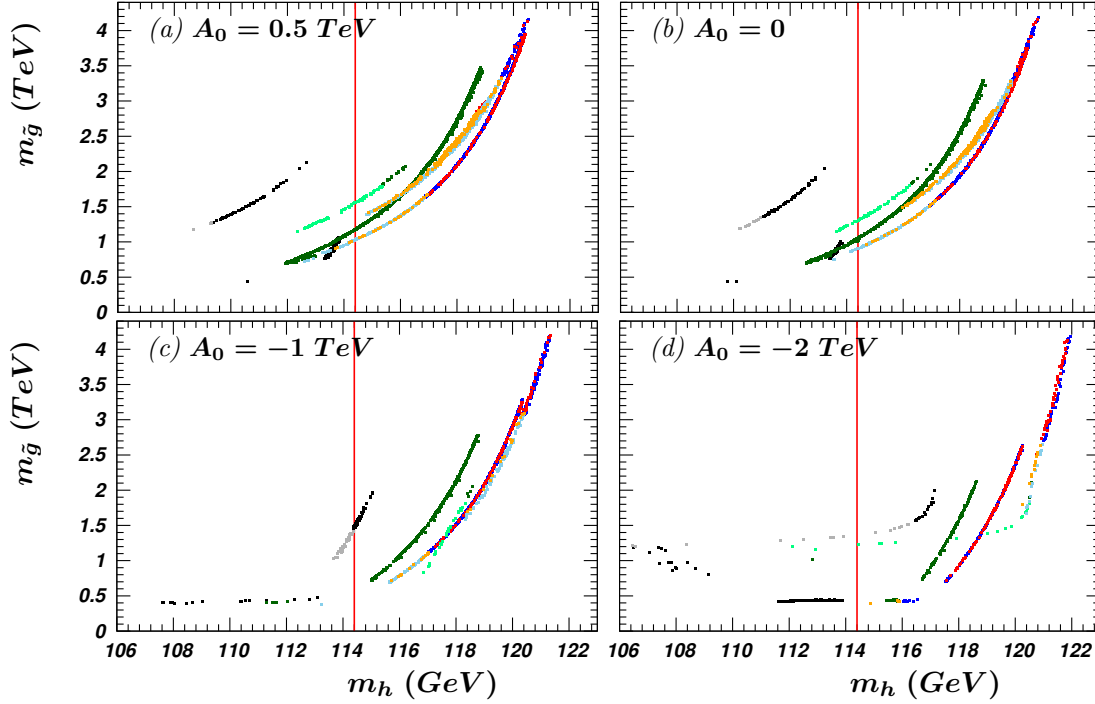


Figure 4: Allowed region for gluino mass versus m_h . The color code is the same as in Fig. 3.

gluino mass [45, 46] do not affect the parameter space left after imposing DM, LEP2 and $b \rightarrow s\gamma$ constraints. On the other hand, the LHC with 100 fb^{-1} luminosity will be able to probe the parameter space corresponding to $m_{\tilde{g}}$ up to $\sim 3 \text{ TeV}$ [88, 90, 99, 100, 101, 102], covering almost the entire $\tilde{\tau}\tilde{Z}$ band. Also, the LHC with 100 fb^{-1} can indirectly probe $m_{\tilde{g}}$ up to $\sim 2.5 \text{ TeV}$ in the HB/FP region via observation of $lepton + jets + \cancel{E}_T$ signal from lighter gauginos [103]. Distinguishing $\tilde{\tau}\tilde{Z}$ and HB/FP bands in $(m_{\tilde{g}}, m_h)$ plane could be somewhat problematic, even though, potentially, the knowledge of the light Higgs boson mass at the percentage level would allow one to indirectly determine the mass of very heavy gluinos with 5 – 10% precision.

In Figs. 5 and 6 we present plots for $m_{\tilde{W}_1}$ versus m_h and $m_{\tilde{Z}_1}$ versus m_h , respectively. The upper band of the allowed parameter space for each particular value of $\tan\beta$ corresponds to the $\tilde{\tau}\tilde{Z}(+\tilde{t}\tilde{Z}+\text{AF})$ region. In this region, the mass of the chargino and the neutralino is being driven up with the rise of $\tan\beta$ up to about $m_{\tilde{W}_1} \simeq 1.7 \text{ TeV}$ and $m_{\tilde{Z}_1} \simeq 850 \text{ GeV}$ for $\tan\beta = 53$. The HB/FP and HF regions are characterized by small $|\mu|$ values resulting in light quasi-degenerate \tilde{Z}_1 and \tilde{W}_1 states. This happens as a result of the following non-trivial interplay of the RG equations. With $m_{1/2}$ fixed, increasing m_0 leads to the suppression of terms with top and bottom Yukawa couplings in the RG equations for m_{H_u} and m_{H_d} . This effect drives the higgs SSB masses towards the “no REWSB” condition and respectively lowers the value of $|\mu|$. These regions form the lower band of the allowed parameter space. The upper tip of this band can reach the mass region as large as $\sim 700 \text{ GeV}$. This limit is defined by the maximal value of $m_0 = 5 \text{ TeV}$ in our scan and practically does not depend on $\tan\beta$. One can see that the slope of the

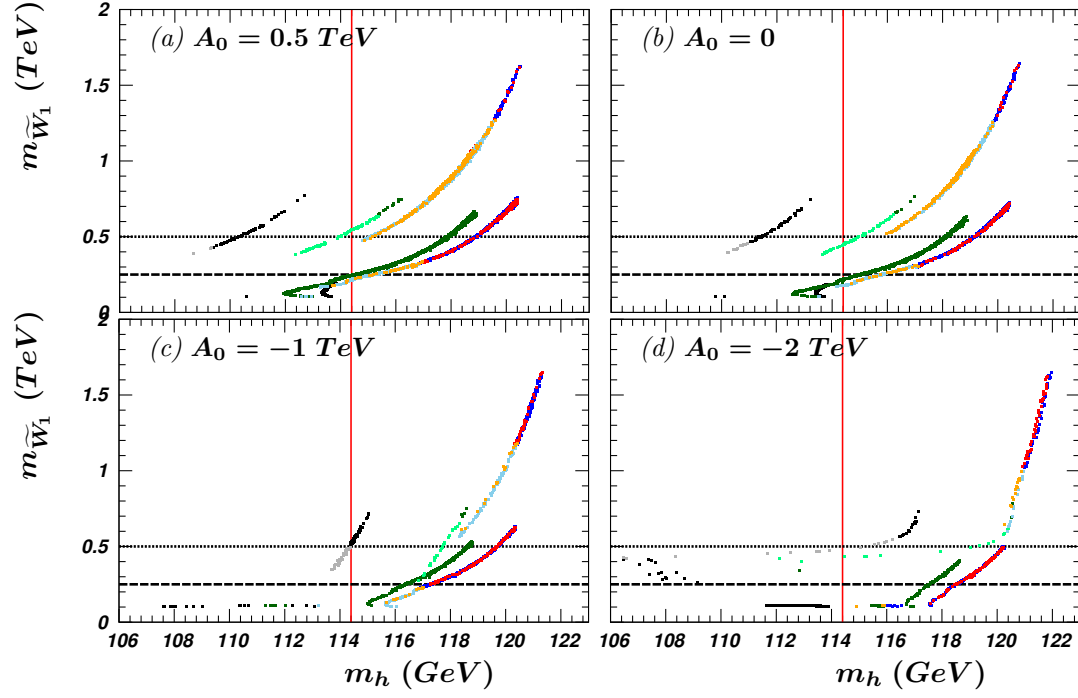


Figure 5: Allowed region for the lightest chargino mass versus m_h . The color code is the same as in Fig. 3. Dashed (dotted) horizontal lines represent approximate reach of ILC500 (ILC1000).

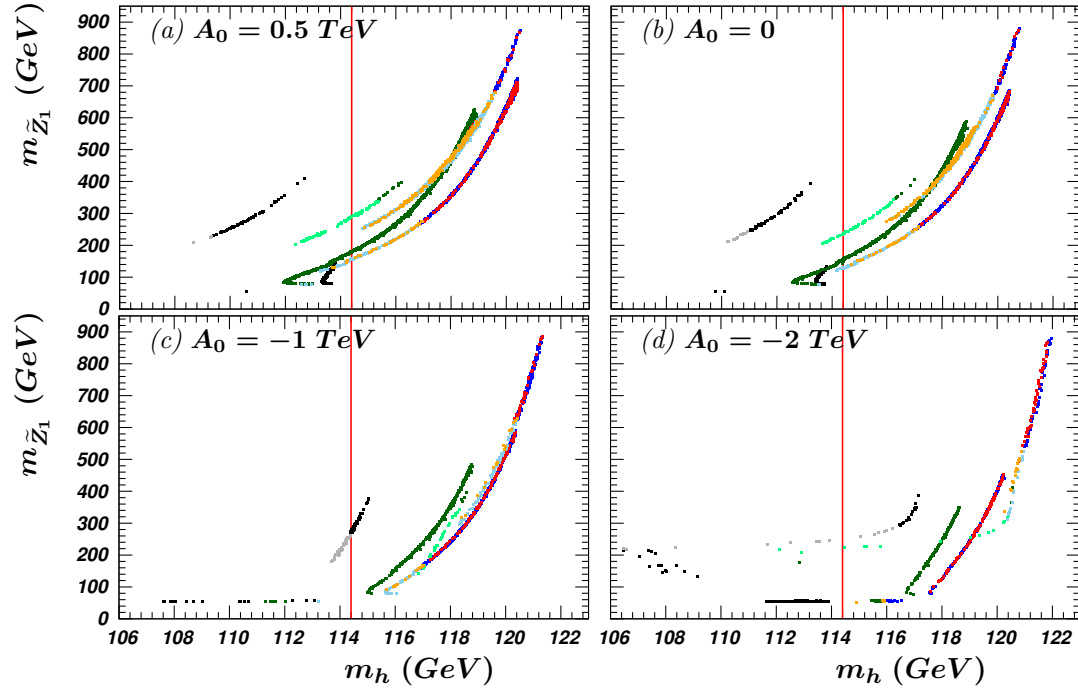


Figure 6: Allowed region for the lightest neutralino mass versus m_h . The color code is the same as in Fig. 3.

coannihilation band is typically larger than the slope of the allowed band of the parameter space corresponding to the focus point region. Therefore, in the coannihilation region one can expect better accuracy in the chargino/neutralino mass determination through the correlations presented in Figs. 5 and 6. Also, using $m_{\tilde{g}} - m_h$ correlation, when the gluino is observed and reconstructed, one can actually predict the chargino and the neutralino masses, whose observation in EW production processes could be problematic. To put things in perspective, we show in Fig. 5 the kinematic limits for $\widetilde{W}_1\widetilde{W}_1$ pair production, which can serve as good approximations for the reach of ILC500 ($\sqrt{s} = 500$ GeV) and ILC1000 ($\sqrt{s} = 1000$ GeV) machines [104, 105, 106]. We see that the linear collider can access only the lower end of the coannihilation band (corresponding to low $m_{1/2}$ values), while the HB/FP region can be probed almost entirely. This is in contrast to the LHC, which has large coverage in the coannihilation region, but can only probe the lower half of the HB/FP region, as was shown in Fig. 4.

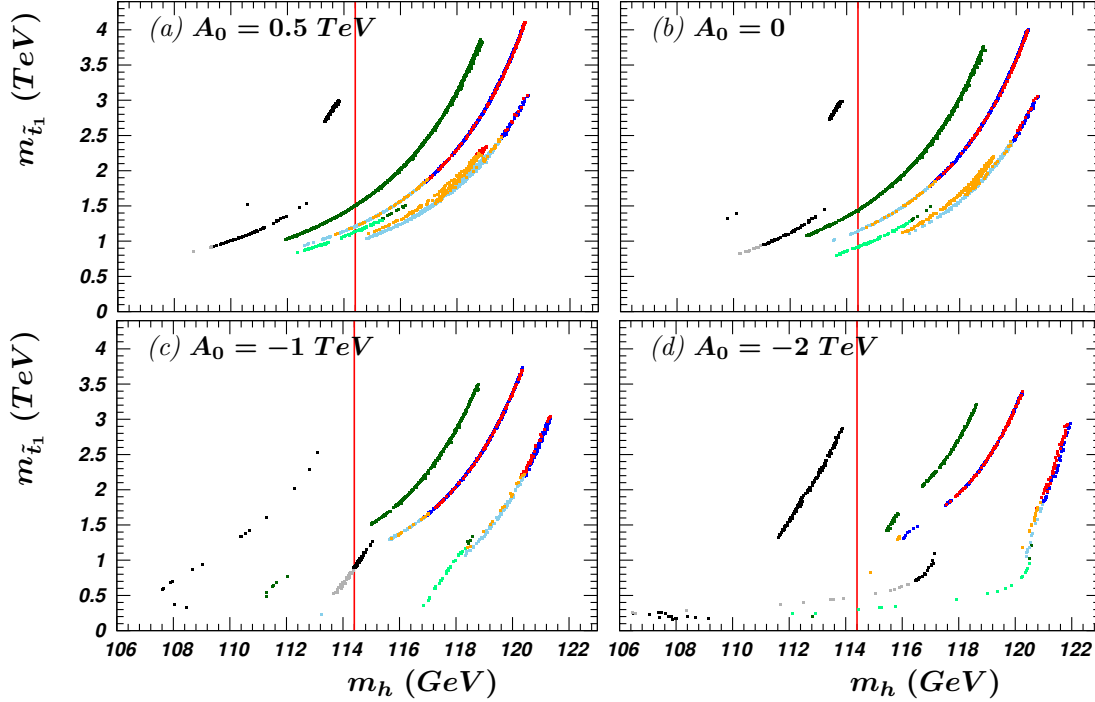


Figure 7: Allowed region for top squark mass mass versus m_h . The color code is the same as in Fig. 3.

In Fig. 7 we present correlations between the lightest top-squark mass and m_h . In this figure, the upper curves for each value of $\tan\beta$ correspond to the HB/FP(+HF) region and the lower curve to the $\tilde{\tau}\tilde{Z}(+\tilde{t}\tilde{Z}+\text{AF})$ region. At $\tan\beta = 53$ and $A_0 = 0.5$ TeV and $A_0 = 0$ in frames a) and b) respectively, one can see that the orange curve is widened in its upper part. This region corresponds to the AF region, where the large range of radiative corrections to the top squark mass and its stronger dependence on various model parameters spoil somewhat the $m_{\tilde{t}_1} - m_h$ correlation. In this region, $m_{\tilde{t}_1} \gtrsim 500$ GeV, thus exceeding the Tevatron bound [47, 48]. One can also notice that for $A_0 = -1$ TeV

and $A_0 = -2$ TeV, presented in frames c) and d), respectively, the top squark exhibiting stop-coannihilation region is allowed to be as light as 200 GeV. This region is represented by the lower tip of the light-green line in frame c), and the lower tips of gray and light-green line in frame d). As A_0 becomes increasingly negative, the mixing between \tilde{t}_L and \tilde{t}_R increases (thereby reducing the mass of \tilde{t}_1) which, in turn, drives m_h to larger values through radiative corrections. This explains why the curves shift to the lower right corner, as we go from frame a) to d).

Let's take a closer look at the 'anatomy' of the stop co-annihilation region. In Fig. 8 we present constraints similar to Figs. 1 and 2, but in the $(m_{\tilde{t}}, m_h)$ plane with the same color coding for $\tan\beta = 30$ and $A_0 = -1$ TeV. The DM-allowed area consists of HB/FP region (upper branch), $\tilde{\tau}\tilde{Z}$ (lower branch), and $\tilde{t}\tilde{Z}$ (the very bottom tip of the DM allowed region) regions. From the frame b) one can clearly notice that the most serious constraint for the stop-coannihilation region comes from the $b \rightarrow s\gamma$. Indeed, for a light top squark, the contribution from the stop-chargino loop increases $Br(b \rightarrow s\gamma)$ beyond the acceptable level. The reason for the appearance of the very small allowed island surrounded by the $b \rightarrow s\gamma$ excluded region is the non-trivial cancellations between stop-chargino and top-charged Higgs loops. Thus, the $\tilde{t}\tilde{Z}$ region does survive in the CMSSM framework, but this scenario is highly constrained.

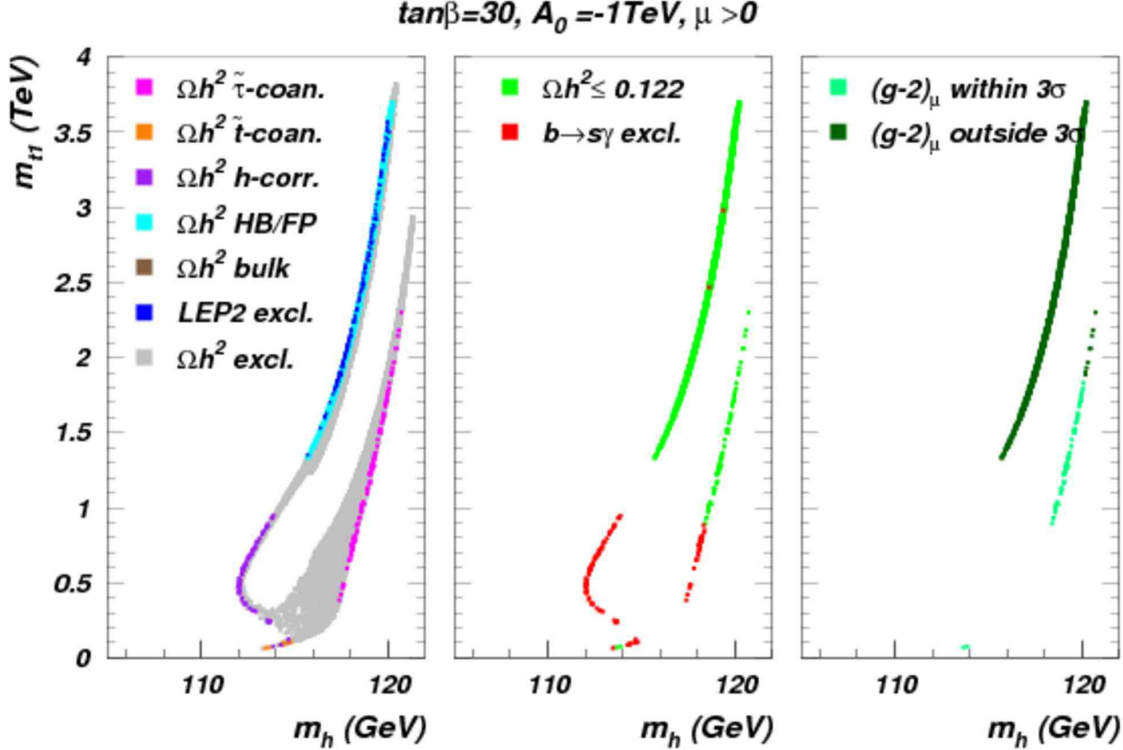


Figure 8: Allowed region for top squark mass mass versus m_h . The color code is the same as in Fig. 1.

Next, in Figs. 9 and 10 we present correlations between the bottom squark mass and m_h , and stau mass and m_h , respectively. One can observe qualitatively similar pattern of

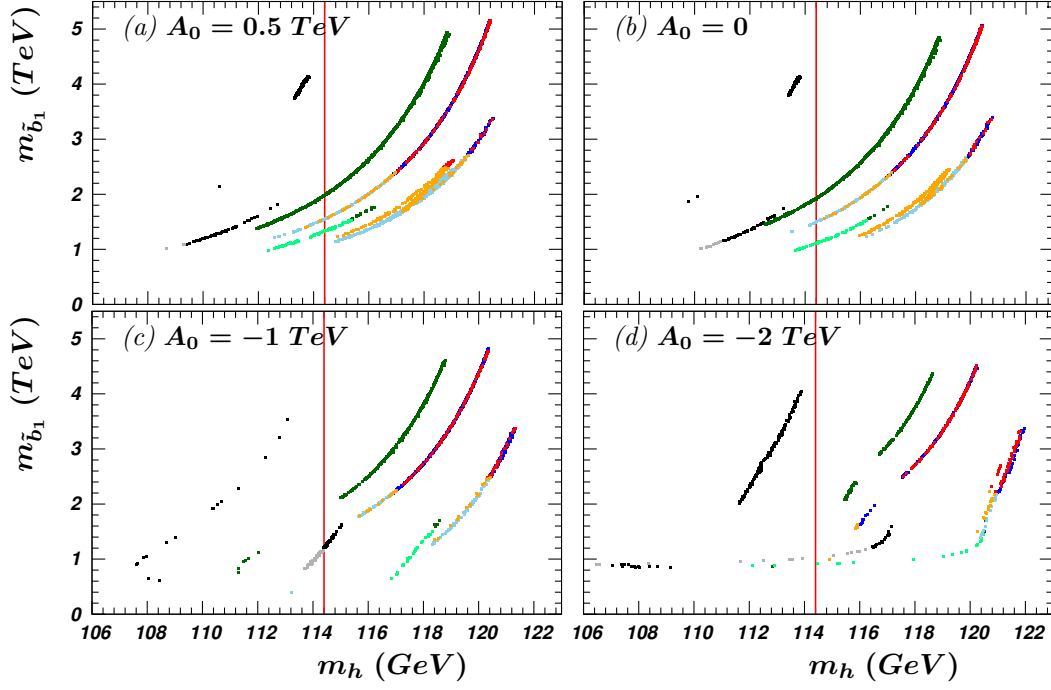


Figure 9: Allowed region for bottom squark mass mass versus m_h . The color code is the same as in Fig. 3.

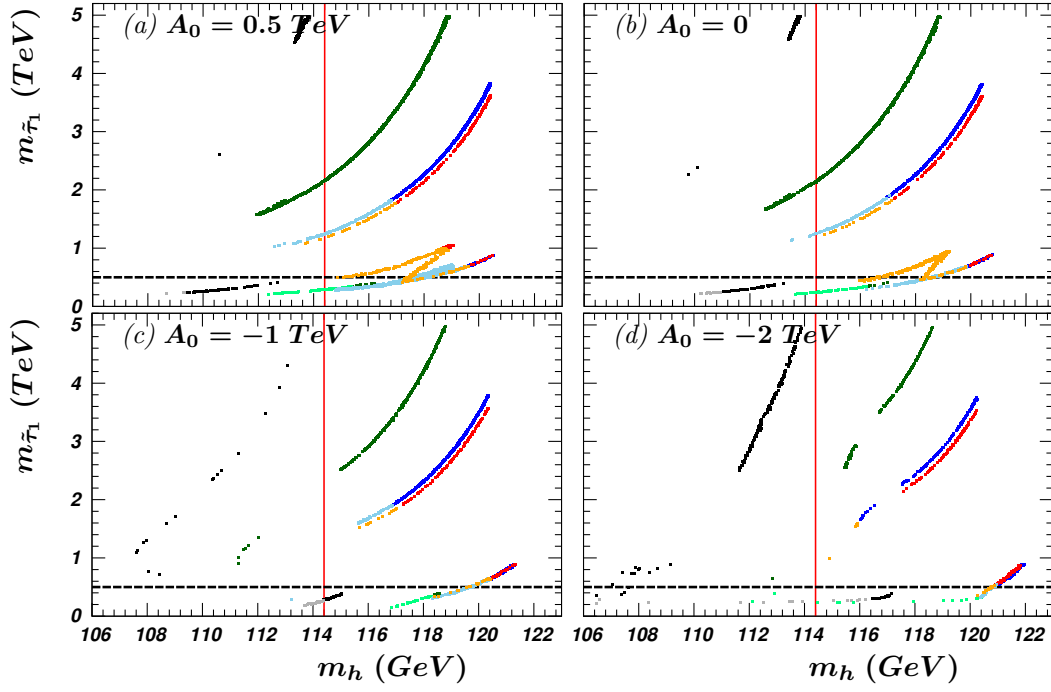


Figure 10: Allowed region for stau mass versus m_h . The color code is the same as in Fig. 3. Dashed horizontal lines represent approximate reach of ILC1000.

correlations in these two figures, where again, as in Fig. 7, the upper curve corresponds to the HB/FP region, while the lower curve corresponds to the stau-coannihilation one. At large $\tan\beta$ and $A_0 = 0.5$ TeV and $A_0 = 0$, the A -funnel region opens up, which is reflected in the behavior of the orange curve. Increasing $\tan\beta$ boosts up the bottom and tau Yukawa couplings, which reduces the sbottom and stau SSB masses through RGE effects, and increases L-R mixing; both effects tend to reduce \tilde{b}_1 and $\tilde{\tau}_1$ masses. This effect is more noticeable for staus, as seen from the wider separation of the HB/FP bands in Fig. 10. Notice that in Fig. 9, the minimal value of bottom squark mass is ~ 500 GeV, which is significantly above the current Tevatron bound [47, 49]. Kinematical limit for $\tilde{W}_1\tilde{W}_1$ pair production at $\sqrt{s} = 1000$ GeV, shown by the dashed horizontal line, indicates an approximate reach of ILC1000 [104, 105, 106].

It is quite informative to also consider the correlation plots for a *fixed value of* $\tan\beta$ and different A_0 values in the same frame. For example, in Fig. 11 we present the allowed

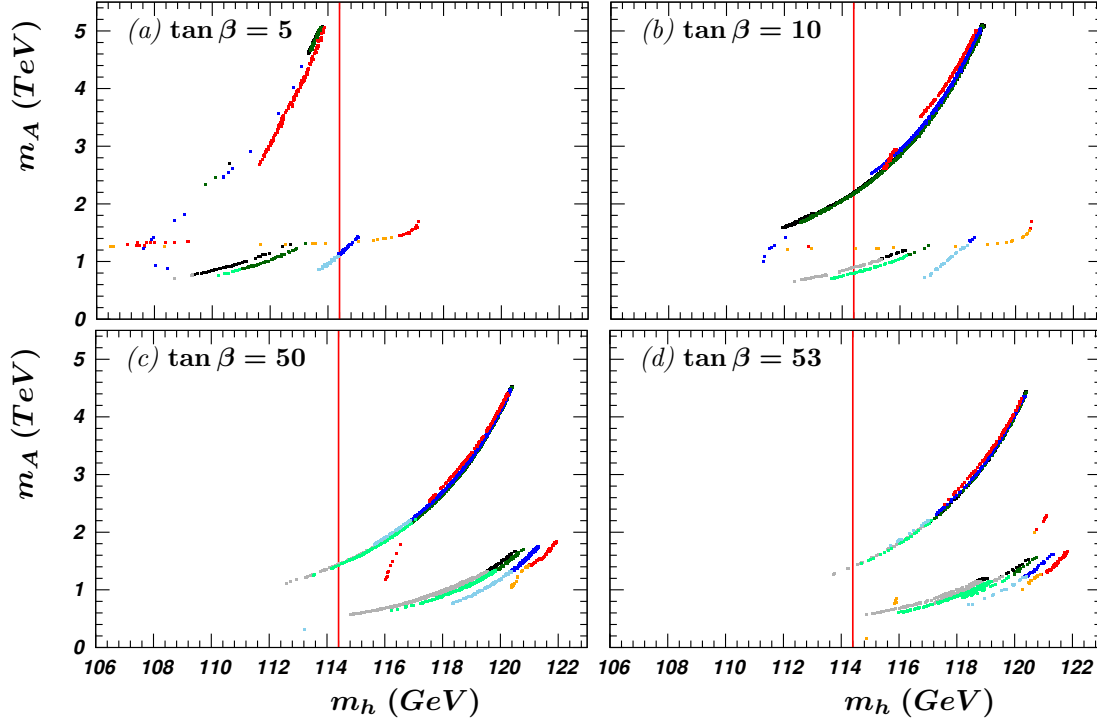


Figure 11: Allowed region for CP-odd Higgs boson mass versus m_h . Gray, light green, light blue, and orange correspond to $A_0 = 0.5, 0, -1$ and -2 TeV, respectively and satisfy 3σ bound on Δa_μ (2.2). Black, dark green, blue and red correspond to $A_0 = 0.5, 0, -1$ and -2 TeV and have Δa_μ outside the 3σ range.

region for the CP-odd Higgs mass versus m_h . Gray, light green, light blue, and orange regions correspond to $A_0 = 0.5, 0, -1$ and -2 TeV respectively and satisfy the 3σ bound (2.2) on Δa_μ ; black, dark green, blue and red colors correspond to regions outside the Δa_μ bound. If we assume that $\tan\beta$ is measured, which can be done at the LHC with an accuracy better than 20% for low to intermediate values of m_A [28], then the strong $m_A - m_h$ correlations above can be used for an indirect prediction of m_A , in case the

CP-odd Higgs boson is too heavy to be directly accessible. A 1% accuracy in the m_h measurement would allow one to estimate m_A with a precision of 5-10%.

One can also use these correlations to determine (or at least strongly constrain) the trilinear coupling A_0 , whose direct measurements are quite problematic. In Fig. 12, we present correlations between the gluino and light higgs boson masses, where we group various A_0 values for fixed $\tan\beta$ in each frame. For each A_0 value, the upper band corresponds to the coannihilation region and the lower one to the HB/FP region. The two groups of bands are very close, but if we discover that we are in the HB/FP or in the coannihilation region, half of the curves will be removed and the remaining ones are well separated for $\tan\beta \gtrsim 10$, which can be used to extract the A_0 value.

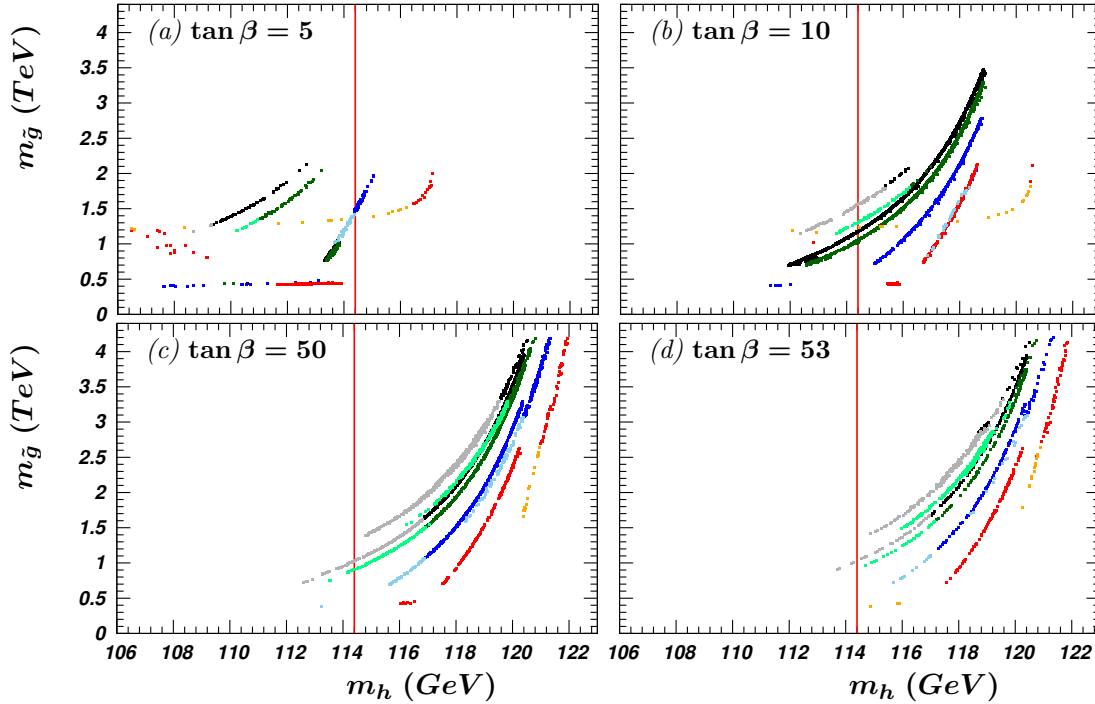


Figure 12: Allowed region for gluino mass versus m_h . The color code is the same as in Fig. 11.

Furthermore, the study of the correlations between various SUSY masses would allow one to further delineate the SUSY parameter space. For example, in Fig. 13 we plot the allowed region in $(m_{\tilde{Z}_1}, m_A)$ plane. We see that the two-fold solution bands form two well separated groups – the lower one representing the coannihilation region and the upper one corresponding to the HB/FP region. One should also notice a third type of bands, namely the vertical one, located at low $m_{\tilde{Z}_1}$ values and corresponding to the HF region. Given m_A (either from direct measurements or extracted from Fig. 11) and $\tan\beta$ values, one can deduce A_0 from the reconstructed neutralino mass. One should point out, however, that the LHC potential can be quite limited in the reconstruction of the heavy neutralino masses in certain regions of the parameter space [102]. Analyzing the direct DM detection (DD) rates, we have found an important complementarity of DM detection experiments in this respect, since these experiments can cover a much wider range of neutralino masses.

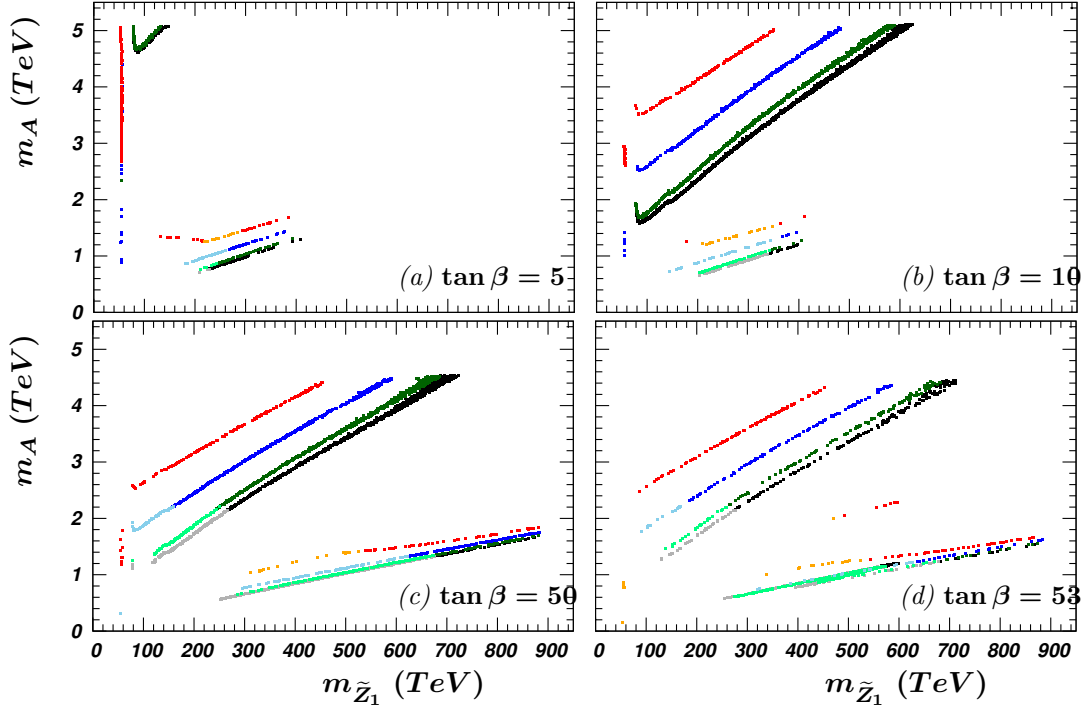


Figure 13: Allowed region for m_A versus $m_{\tilde{Z}_1}$. The color code is the same as in Fig. 11.

In Fig. 14, we present the DD rates, in detector-invariant way, as spin-independent neutralino-proton elastic scattering cross section versus the neutralino mass. We used IsaReS code [107], a part of IsaTools package, with pion-nucleon Σ term assumed to be 45 MeV⁶. One can clearly read patterns coming from different dark matter motivated regions. The upper band corresponds to HB/FP region, where \tilde{Z}_1 has a substantial higgsino component thereby enhancing its scattering cross section off the proton. The lower pattern comes from the stau coannihilation region (merging with A-funnel for $\tan\beta = 53$). We see that the HB/FP and coannihilation regions are always separated in terms of spin-independent cross section. One should also note the h-funnel region, which is represented by narrow vertical band at $m_{\tilde{Z}_1} \sim 55$ GeV. This region is well separated from HB/FP and $\tilde{\tau}\tilde{Z}$ regions and could be almost completely covered by XENON 1 ton detector.

The current best limit comes from the XENON-10 collaboration [109], which obtained an upper limit $\sigma_{SI}(\tilde{Z}_1 p) \lesssim 8 \times 10^{-8}$ pb for $m_{\tilde{Z}_1} \sim 100$ GeV. We also show the projection for CDMS2 [110], which is expected to release results next year, and for its planned upgrade, SuperCDMS [111]. The reach of XENON-1 ton detector as representative of many planned large noble gas detectors [112, 113, 114, 115] aiming for a sensitivity of $\sim 10^{-10}$ pb is presented as well. One can see that Stage-2 detectors, like SuperCDMS, and eventually Stage-3 detectors, like XENON-1 ton, will be able to observe the signal from neutralino scattering off the nuclei in the entire HB/FP region and measure the respective

⁶Recent experimental results suggest a somewhat different value of the Σ term than the canonical value we assumed in this work. This affects the contribution from s-quark diagrams and can change our predictions for $\sigma_{SI}(\tilde{Z}_1 p)$ by about a factor of three [108].

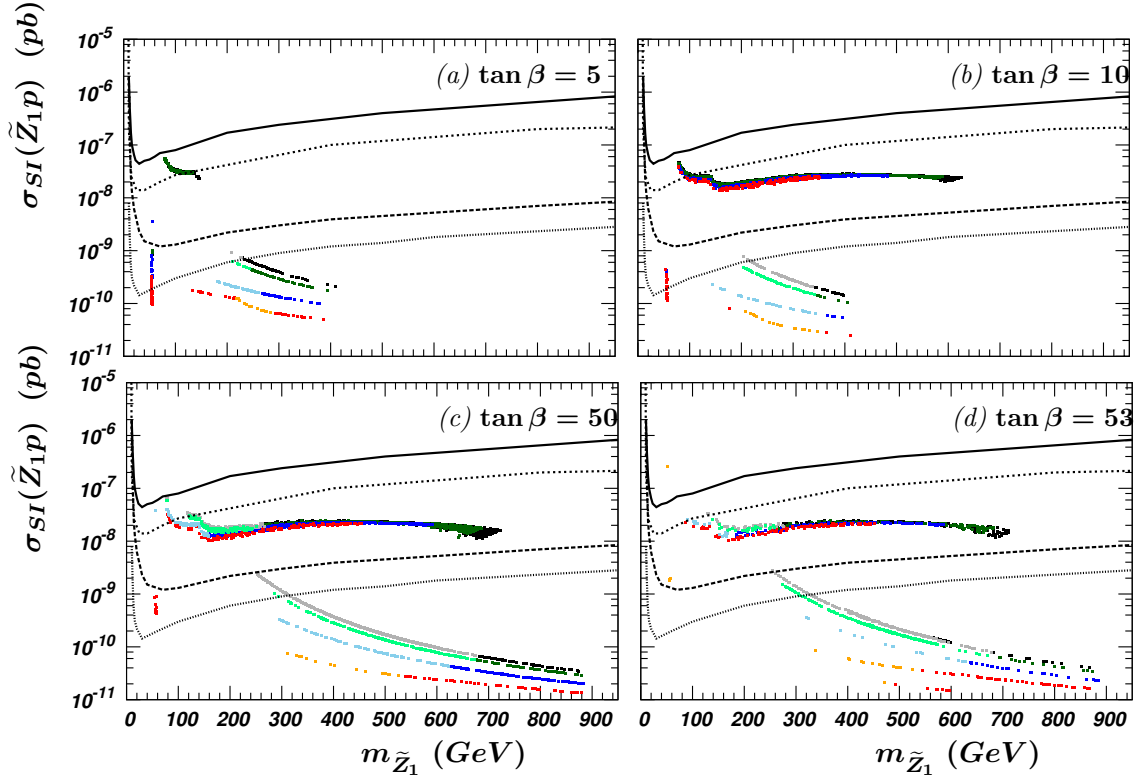


Figure 14: Allowed region for spin-independent neutralino scattering cross section on proton plotted versus $m_{\tilde{Z}_1}$. The color code is the same as in Fig. 11. We also show the reach and projected reach of XENON-10, CDMS-II, SuperCDMS and XENON-1 ton detectors by solid, dashed, long-dashed and dotted lines, respectively.

neutralino mass exhibiting the prominent complementarity to LHC. Observation of the signal in CDMS2 or a Stage-2 detector will clearly be an indication of the HB/FP region. These results can be used in conjunction, for example, with the LHC results for $m_{\tilde{g}}$ and m_h to determine A_0 from Fig. 12, since the ambiguity of the HB/FP and the coannihilation region curves could be resolved using DD results. Also, positive result from DM searches will provide us with the neutralino mass, which, in turn, can be employed to extract A_0 from the correlations of Fig. 13. If the sensitivity of DD experiments would be further increased to $\sim 10^{-10} - 10^{-11}$ pb level, then individual curves from the stau-coannihilation pattern in Fig. 14 could be resolved and one could probe the A_0 parameter in this region.

4. Conclusion

We have performed an updated scan of the CMSSM parameter space, taking into account the revised (lower) value of top quark mass, updated SUSY constraints from collider and low energy physics as well as crucial constraint on dark matter abundance from WMAP3. The scan was performed in the CMSSM parameter space for $\mu > 0$, and for a plausible range of values for m_0 , $m_{1/2}$ and $|A_0|$ and for $\tan\beta = 5, 10, 50$ and 53 .

We have demonstrated that taking account of the SUSY constraints, especially the dark matter abundance, strong correlations occur between the sparticle and Higgs masses.

The correlations between the light CP-even Higgs boson mass and SUSY particles could potentially allow determination of the sparticle spectra with a few percent accuracy, assuming a theoretical control of m_h at the percent level. All correlations we have found are represented by separated narrow bands, two-fold solutions which exhibit focus point and h-funnel regions, or co-annihilation and A-funnel regions respectively.

The correlations found among the sparticle and Higgs masses would also allow one to delineate the value of the trilinear coupling which can potentially be large. The large value of the trilinear coupling A_0 is especially motivated by the present light Higgs mass constraints and the latest top-quark mass measurements. Since the top quark world-averaged mass went down to 170.9 GeV, the additional contributions from A_t and A_b are even more important to increase m_h and thereby overcome the LEP2 limit. We have found that even for a parameter space with m_0 and $|A_0|$ as large as 5 TeV and 2 TeV respectively at M_{GUT} , the lightest Higgs boson mass is limited by 122-123 GeV from above.

We have found that some correlations, like between (m_A, m_h) , $(m_A, m_{\tilde{g}})$ and $(m_A, m_{\tilde{Z}_1})$ could allow one to reveal the value of A_0 and help to distinguish the DM motivated band of the parameter space mentioned above. Moreover, we have demonstrated striking complementarity between the LHC and direct dark matter detection experiments in resolving the SUSY mass spectrum and determination of SUSY parameters. Stage 2 experiments like SuperCDMS will be able to cover the entire HB/FP region and resolve the ambiguity of HB/FP and non-HB/FP bands for several important correlations.

The correlations we have presented in this paper can be a useful input for SUSY global analysis fit as well as for experimental delineation of the SUSY parameter space. We would also like to emphasize that including the experimental input both from collider physics and from dark matter detection experiments would allow one to significantly improve the understanding of the SUSY spectrum and the underlying parameter space.

Acknowledgments

We thank H. Baer, X. Tata and A. Djouadi for useful discussions. This work is supported in part by grants from the US Department of Energy, S.D., I.G., and Q.S. (Grant # DE-FG02-91ER40626) and A.M. (Grant # DE-FG02-04ER41308). S.D. was also supported by the University of Delaware competitive fellowship. A.B. acknowledges partial support from PPARC Rolling Grant PPA/G/S/2003/00096.

References

- [1] **Tevatron Electroweak Working Group** , *A combination of CDF and D0 results on the mass of the top quark*, [hep-ex/0703034](#).
- [2] **ALEPH, DELPHI, L3 and OPAL Collaborations and LEP Working Group for Higgs Boson Searches** , S. Schael *et. al.*, *Search for neutral MSSM higgs bosons at LEP*, *Eur. Phys. J.* **C47** (2006) 547–587, [[hep-ex/0602042](#)].
- [3] A. H. Chamseddine, R. Arnowitt, and P. Nath, *Locally supersymmetric grand unification*, *Phys. Rev. Lett.* **49** (1982) 970.

- [4] R. Barbieri, S. Ferrara, and C. A. Savoy, *Gauge models with spontaneously broken local supersymmetry*, *Phys. Lett.* **B119** (1982) 343.
- [5] L. J. Hall, J. D. Lykken, and S. Weinberg, *Supergravity as the messenger of supersymmetry breaking*, *Phys. Rev.* **D27** (1983) 2359–2378.
- [6] E. Cremmer, P. Fayet, and L. Girardello, *Gravity induced supersymmetry breaking and low-energy mass spectrum*, *Phys. Lett.* **B122** (1983) 41.
- [7] N. Ohta, *Grand unified theories based on local supersymmetry*, *Prog. Theor. Phys.* **70** (1983) 542.
- [8] H. Baer *et. al.*, *Updated constraints on the minimal supergravity model*, *JHEP* **07** (2002) 050, [[hep-ph/0205325](#)].
- [9] H. Baer and C. Balazs, *χ^2 analysis of the minimal supergravity model including WMAP, $g(\mu)-2$ and $b \rightarrow s$ gamma constraints*, *JCAP* **0305** (2003) 006, [[hep-ph/0303114](#)].
- [10] U. Chattopadhyay, A. Corsetti, and P. Nath, *WMAP constraints, SUSY dark matter and implications for the direct detection of SUSY*, *Phys. Rev.* **D68** (2003) 035005, [[hep-ph/0303201](#)].
- [11] J. R. Ellis, K. A. Olive, Y. Santoso, and V. C. Spanos, *Supersymmetric dark matter in light of WMAP*, *Phys. Lett.* **B565** (2003) 176–182, [[hep-ph/0303043](#)].
- [12] M. Battaglia *et. al.*, *Updated post-WMAP benchmarks for supersymmetry*, *Eur. Phys. J.* **C33** (2004) 273–296, [[hep-ph/0306219](#)].
- [13] R. Arnowitt, B. Dutta, and B. Hu, *Dark matter, muon $g-2$ and other SUSY constraints*, [[hep-ph/0310103](#)].
- [14] J. R. Ellis, K. A. Olive, Y. Santoso, and V. C. Spanos, *Likelihood analysis of the CMSSM parameter space*, *Phys. Rev.* **D69** (2004).
- [15] H. Baer, A. Belyaev, T. Krupovnickas, and A. Mustafayev, *SUSY normal scalar mass hierarchy reconciles $(g-2)(\mu)$, $b \rightarrow s$ gamma and relic density*, *JHEP* **06** (2004) 044, [[hep-ph/0403214](#)].
- [16] M. E. Gomez, T. Ibrahim, P. Nath, and S. Skadhauge, *Sensitivity of supersymmetric dark matter to the b quark mass*, *Phys. Rev.* **D70** (2004) 035014, [[hep-ph/0404025](#)].
- [17] J. R. Ellis, S. Heinemeyer, K. A. Olive, and G. Weiglein, *Indirect sensitivities to the scale of supersymmetry*, *JHEP* **02** (2005) 013, [[hep-ph/0411216](#)].
- [18] W. de Boer *et al.*, *Combined Fit of Low Energy Constraints to Minimal Supersymmetry and Discovery Potential at LEP II*, *Z. Phys.* **C71** (1996) 415–430, [[hep-ph/9603350](#)].
- [19] **Tevatron Electroweak Working Group**, E. Brubaker *et. al.*, *Combination of CDF and D0 results on the mass of the top quark*, [[hep-ex/0608032](#)].
- [20] J. R. Ellis, D. V. Nanopoulos, K. A. Olive, and Y. Santoso, *On the higgs mass in the CMSSM*, *Phys. Lett.* **B633** (2006) 583–590, [[hep-ph/0509331](#)].
- [21] A. Djouadi, M. Drees, and J.-L. Kneur, *Updated constraints on the minimal supergravity model*, *JHEP* **03** (2006) 033, [[hep-ph/0602001](#)].
- [22] J. Ellis, T. Hahn, S. Heinemeyer, K. A. Olive, and G. Weiglein, *WMAP-compliant benchmark surfaces for MSSM higgs bosons*, [arXiv:0709.0098](#).

- [23] L. Roszkowski, R. Ruiz de Austri and R. Trotta, *Implications for the Constrained MSSM from a new prediction for b to s gamma*, *JHEP* **07** (2007) 075, [[arXiv:0705.2012](#)].
- [24] H. Baer and X. Tata, *Weak scale supersymmetry: From superfields to scattering events*, Cambridge, UK: Univ. Pr. (2006) 537 p.
- [25] J. R. Ellis, K. A. Olive, Y. Santoso, and V. C. Spanos, *Phenomenological constraints on patterns of supersymmetry breaking*, *Phys. Lett.* **B573** (2003) 162–172, [[hep-ph/0305212](#)].
- [26] J. R. Ellis, K. A. Olive, Y. Santoso, and V. C. Spanos, *Very constrained minimal supersymmetric standard models*, *Phys. Rev.* **D70** (2004) 055005, [[hep-ph/0405110](#)].
- [27] M. Drees, R. Godbole, and P. Roy, *Theory and phenomenology of sparticles: An account of four- dimensional $N=1$ supersymmetry in high energy physics*, . Hackensack, USA: World Scientific (2004) 555 p.
- [28] **ATLAS** Collaboration, *Atlas detector and physics performance. Technical design report. vol. 2*, CERN-LHCC-99-15.
- [29] **CMS** Collaboration, *CMS physics technical design report, volume ii: Physics performance*, *J. Phys. G: Nucl. Part. Phys.* **34** (2007) 995–1579.
- [30] S. P. Martin, *Three-loop corrections to the lightest higgs scalar boson mass in supersymmetry*, *Phys. Rev.* **D75** (2007) 055005, [[hep-ph/0701051](#)].
- [31] G. F. Giudice and A. Romanino, *Split supersymmetry*, *Nucl. Phys.* **B699** (2004) 65–89, [[hep-ph/0406088](#)].
- [32] H. Baer, F. E. Paige, S. D. Protopopescu, and X. Tata, *Isajet 7.48: A monte carlo event generator for $p p$, $anti-p p$, and $e+ e-$ reactions*, [hep-ph/0001086](#).
- [33] J. Hisano, H. Murayama, and T. Yanagida, *Nucleon decay in the minimal supersymmetric $SU(5)$ grand unification*, *Nucl. Phys.* **B402** (1993) 46–84, [[hep-ph/9207279](#)].
- [34] Y. Yamada, *SUSY and GUT threshold effects in SUSY $SU(5)$ models*, *Z. Phys.* **C60** (1993) 83–94.
- [35] D. M. Pierce, J. A. Bagger, K. T. Matchev, and R.-j. Zhang, *Precision corrections in the minimal supersymmetric standard model*, *Nucl. Phys.* **B491** (1997) 3–67, [[hep-ph/9606211](#)].
- [36] H. Baer, J. Ferrandis, S. Kraml, and W. Porod, *On the treatment of threshold effects in SUSY spectrum computations*, *Phys. Rev.* **D73** (2006) 015010, [[hep-ph/0511123](#)].
- [37] S. Heinemeyer, W. Hollik, and G. Weiglein, *FeynHiggsFast: A program for a fast calculation of masses and mixing angles in the higgs sector of the MSSM*, [hep-ph/0002213](#).
- [38] L. E. Ibanez and G. G. Ross, *$SU(2)_L \times U(1)$ symmetry breaking as a radiative effect of supersymmetry breaking in GUTs*, *Phys. Lett.* **B110** (1982) 215–220.
- [39] L. E. Ibanez, *Locally supersymmetric $SU(5)$ grand unification*, *Phys. Lett.* **B118** (1982) 73.
- [40] J. R. Ellis, D. V. Nanopoulos, and K. Tamvakis, *Grand unification in simple supergravity*, *Phys. Lett.* **B121** (1983) 123.
- [41] L. Alvarez-Gaume, J. Polchinski, and M. B. Wise, *Minimal low-energy supergravity*, *Nucl. Phys.* **B221** (1983) 495.
- [42] **Particle Data Group** , W. M. Yao *et. al.*, *Review of particle physics*, *J. Phys.* **G33** (2006) 1–1232.

- [43] **LEP2 SUSY Working Group**, *Combined LEP selectron/smuon/stau results, 183-208 GeV*,
http://lepsusy.web.cern.ch/lepsusy/www/sleptons_summer04/slep_final.html.
- [44] **LEP2 SUSY Working Group**, *Combined LEP chargino results, up to 208 GeV for large m_0* , http://lepsusy.web.cern.ch/lepsusy/www/inos_moriond01/charginos_pub.html.
- [45] **CDF Collaboration**, *Search for squark/gluino production in met+jets final state (1.4 fb^{-1})*,
http://www-cdf.fnal.gov/physics/exotic/r2a/20070809.squark_gluino/public.html.
- [46] **D0 Collaboration**, *Search for squarks and gluinos in events with jets and missing E_t (960 pb^{-1})*, D0 note 5312, see
<http://www-d0.fnal.gov/Run2Physics/WWW/results/prelim/NP/N50/>.
- [47] **CDF Collaboration**, T. Aaltonen *et. al.*, *Search for direct pair production of supersymmetric top and supersymmetric bottom quarks in $p\bar{p}$ collisions at $\sqrt{s} = 1.96 \text{ TeV}$* ,
arXiv:0707.2567.
- [48] **D0 Collaboration**, *Search for scalar top quarks in acoplanar charm jet + missing energy events (995 pb^{-1})*, D0 note 5436, see
<http://www-d0.fnal.gov/Run2Physics/WWW/results/prelim/NP/N56/>.
- [49] **D0 Collaboration**, V. M. Abazov *et. al.*, *Search for pair production of scalar bottom quarks in p anti- p collisions at $s^{*(1/2)} = 1.96 \text{ TeV}$* , *Phys. Rev. Lett.* **97** (2006) 171806,
[hep-ex/0608013].
- [50] A. Belyaev, Q.-H. Cao, D. Nomura, K. Tobe, and C. P. Yuan, *Light MSSM higgs boson scenario and its test at hadron colliders*, hep-ph/0609079.
- [51] M. Drees, *Neutralino dark matter in 2005*, *AIP Conf. Proc.* **805** (2006) 48–54,
[hep-ph/0509105].
- [52] **WMAP Collaboration**, D. N. Spergel *et. al.*, *Wilkinson microwave anisotropy probe (WMAP) three year results: Implications for cosmology*, *Astrophys. J. Suppl.* **170** (2007) 377, [astro-ph/0603449].
- [53] M. Drees, H. Iminniyaz, and M. Kakizaki, *Abundance of cosmological relics in low-temperature scenarios*, *Phys. Rev.* **D73** (2006) 123502, [hep-ph/0603165].
- [54] H. Baer, C. Balazs, and A. Belyaev, *Neutralino relic density in minimal supergravity with co-annihilations*, *JHEP* **03** (2002) 042, [hep-ph/0202076].
- [55] A. Pukhov *et. al.*, *Comphep: A package for evaluation of feynman diagrams and integration over multi-particle phase space. User's manual for version 33*, hep-ph/9908288.
- [56] **CompHEP Collaboration**, E. Boos *et. al.*, *Comphep 4.4: Automatic computations from lagrangians to events*, *Nucl. Instrum. Meth.* **A534** (2004) 250–259, [hep-ph/0403113].
- [57] **Muon G-2 Collaboration**, G. W. Bennett *et. al.*, *Final report of the muon E821 anomalous magnetic moment measurement at bnl*, *Phys. Rev.* **D73** (2006) 072003, [hep-ex/0602035].
- [58] M. Davier, *The hadronic contribution to $(g-2)(\mu)$* , *Nucl. Phys. Proc. Suppl.* **169** (2007) 288–296, [hep-ph/0701163].
- [59] K. Hagiwara, A. D. Martin, D. Nomura, and T. Teubner, *Improved predictions for $g-2$ of the muon and $\alpha_{\text{qed}}(m_z^2)$* , *Phys. Lett.* **B649** (2007) 173–179, [hep-ph/0611102].

- [60] D. W. Hertzog, J. P. Miller, E. de Rafael, B. Lee Roberts, and D. Stockinger, *The physics case for the new muon ($g-2$) experiment*, [arXiv:0705.4617](#).
- [61] J. P. Miller, E. de Rafael, and B. L. Roberts, *Muon $g-2$: Review of theory and experiment*, *Rept. Prog. Phys.* **70** (2007) 795, [[hep-ph/0703049](#)].
- [62] H. Baer, C. Balazs, J. Ferrandis, and X. Tata, *Impact of muon anomalous magnetic moment on supersymmetric models*, *Phys. Rev.* **D64** (2001) 035004, [[hep-ph/0103280](#)].
- [63] H. Baer and M. Brhlik, *QCD improved $b \rightarrow s$ gamma constraints on the minimal supergravity model*, *Phys. Rev.* **D55** (1997) 3201–3208, [[hep-ph/9610224](#)].
- [64] H. Baer, M. Brhlik, D. Castano, and X. Tata, *$b \rightarrow s$ gamma constraints on the minimal supergravity model with large $\tan(\beta)$* , *Phys. Rev.* **D58** (1998) 015007, [[hep-ph/9712305](#)].
- [65] **Heavy Flavor Averaging Group (HFAG)**, E. Barberio *et. al.*, *Averages of b -hadron properties at the end of 2005*, [hep-ex/0603003](#). For a very recent update see Heavy Flavor Averaging Group (HFAG) (E. Barberio *et al.*), *Averages of b -hadron properties at the end of 2006*, [arXiv:0704.3575](#).
- [66] M. Misiak, *NNLO QCD corrections to $b \rightarrow x/s$ gamma*, [hep-ph/0609289](#).
- [67] M. Misiak and M. Steinhauser, *NNLO QCD corrections to the anti- $b \rightarrow x/s$ gamma matrix elements using interpolation in $m(c)$* , *Nucl. Phys.* **B764** (2007) 62–82, [[hep-ph/0609241](#)].
- [68] P. Gambino and M. Misiak, *Quark mass effects in anti- $b \rightarrow x/s$ gamma*, *Nucl. Phys.* **B611** (2001) 338–366, [[hep-ph/0104034](#)].
- [69] **CDF Collaboration**. CDF note 8176, see <http://www-cdf.fnal.gov/physics/new/bottom/060316.blessed-bsmumu3/>.
- [70] J. K. Mizukoshi, X. Tata, and Y. Wang, *Higgs-mediated leptonic decays of B_s and B_d mesons as probes of supersymmetry*, *Phys. Rev.* **D66** (2002) 115003, [[hep-ph/0208078](#)].
- [71] J. R. Ellis, J. S. Hagelin, D. V. Nanopoulos, and M. Srednicki, *Search for supersymmetry at the anti- p p collider*, *Phys. Lett.* **B127** (1983) 233.
- [72] J. R. Ellis, J. S. Hagelin, D. V. Nanopoulos, K. A. Olive, and M. Srednicki, *Supersymmetric relics from the big bang*, *Nucl. Phys.* **B238** (1984) 453–476.
- [73] H. Baer and M. Brhlik, *Cosmological relic density from minimal supergravity with implications for collider physics*, *Phys. Rev.* **D53** (1996) 597–605, [[hep-ph/9508321](#)].
- [74] V. D. Barger and C. Kao, *Relic density of neutralino dark matter in supergravity models*, *Phys. Rev.* **D57** (1998) 3131–3139, [[hep-ph/9704403](#)].
- [75] J. R. Ellis, T. Falk, and K. A. Olive, *Neutralino stau coannihilation and the cosmological upper limit on the mass of the lightest supersymmetric particle*, *Phys. Lett.* **B444** (1998) 367–372, [[hep-ph/9810360](#)].
- [76] J. R. Ellis, T. Falk, K. A. Olive, and M. Srednicki, *Calculations of neutralino stau coannihilation channels and the cosmologically relevant region of MSSM parameter space*, *Astropart. Phys.* **13** (2000) 181–213, [[hep-ph/9905481](#)].
- [77] M. E. Gomez, G. Lazarides, and C. Pallis, *Supersymmetric cold dark matter with yukawa unification*, *Phys. Rev.* **D61** (2000) 123512, [[hep-ph/9907261](#)].
- [78] M. E. Gomez, G. Lazarides, and C. Pallis, *Yukawa unification, $b \rightarrow s$ gamma and bino stau coannihilation*, *Phys. Lett.* **B487** (2000) 313–320, [[hep-ph/0004028](#)].

- [79] B. Ananthanarayan, G. Lazarides, and Q. Shafi, *Radiative electroweak breaking and sparticle spectroscopy with $\tan \beta$ approximately $= m(t) / m(b)$* , *Phys. Lett.* **B300** (1993) 245–250.
- [80] B. Ananthanarayan, Q. Shafi, and X. M. Wang, *Improved predictions for top quark, lightest supersymmetric particle, and higgs scalar masses*, *Phys. Rev.* **D50** (1994) 5980–5984, [[hep-ph/9311225](#)].
- [81] A. B. Lahanas, D. V. Nanopoulos, and V. C. Spanos, *Neutralino relic density in a universe with non-vanishing cosmological constant*, *Phys. Rev.* **D62** (2000) 023515, [[hep-ph/9909497](#)].
- [82] R. Arnowitt, B. Dutta, and Y. Santoso, *Coannihilation effects in supergravity and D-brane models*, *Nucl. Phys.* **B606** (2001) 59–83, [[hep-ph/0102181](#)].
- [83] C. Boehm, A. Djouadi, and M. Drees, *Light scalar top quarks and supersymmetric dark matter*, *Phys. Rev.* **D62** (2000) 035012, [[hep-ph/9911496](#)].
- [84] J. R. Ellis, K. A. Olive, and Y. Santoso, *Calculations of neutralino stop coannihilation in the CMSSM*, *Astropart. Phys.* **18** (2003) 395–432, [[hep-ph/0112113](#)].
- [85] J. Edsjo, M. Schelke, P. Ullio, and P. Gondolo, *Accurate relic densities with neutralino, chargino and sfermion coannihilations in mSUGRA*, *JCAP* **0304** (2003) 001, [[hep-ph/0301106](#)].
- [86] K. L. Chan, U. Chattopadhyay, and P. Nath, *Naturalness, weak scale supersymmetry and the prospect for the observation of supersymmetry at the Tevatron and at the LHC*, *Phys. Rev.* **D58** (1998) 096004, [[hep-ph/9710473](#)].
- [87] J. L. Feng, K. T. Matchev, and T. Moroi, *Multi-TeV scalars are natural in minimal supergravity*, *Phys. Rev. Lett.* **84** (2000) 2322–2325, [[hep-ph/9908309](#)].
- [88] H. Baer, C.-h. Chen, F. Paige, and X. Tata, *Signals for minimal supergravity at the CERN large hadron collider: Multi - jet plus missing energy channel*, *Phys. Rev.* **D52** (1995) 2746–2759, [[hep-ph/9503271](#)].
- [89] H. Baer, C.-h. Chen, F. Paige, and X. Tata, *Signals for minimal supergravity at the CERN large hadron collider ii: Multilepton channels*, *Phys. Rev.* **D53** (1996) 6241–6264, [[hep-ph/9512383](#)].
- [90] H. Baer, C.-h. Chen, M. Drees, F. Paige, and X. Tata, *Probing minimal supergravity at the CERN LHC for large $\tan(\beta)$* , *Phys. Rev.* **D59** (1999) 055014, [[hep-ph/9809223](#)].
- [91] P. Nath and R. Arnowitt, *Predictions in $SU(5)$ supergravity grand unification with proton stability and relic density constraints*, *Phys. Rev. Lett.* **70** (1993) 3696–3699, [[hep-ph/9302318](#)].
- [92] M. Drees and M. M. Nojiri, *The neutralino relic density in minimal $N=1$ supergravity*, *Phys. Rev.* **D47** (1993) 376–408, [[hep-ph/9207234](#)].
- [93] H. Baer and M. Brhlik, *Neutralino dark matter in minimal supergravity: Direct detection vs. collider searches*, *Phys. Rev.* **D57** (1998) 567–577, [[hep-ph/9706509](#)].
- [94] H. Baer *et. al.*, *Yukawa unified supersymmetric $SO(10)$ model: Cosmology, rare decays and collider searches*, *Phys. Rev.* **D63** (2001) 015007, [[hep-ph/0005027](#)].
- [95] J. R. Ellis, T. Falk, G. Ganis, K. A. Olive, and M. Srednicki, *The CMSSM parameter space at large $\tan(\beta)$* , *Phys. Lett.* **B510** (2001) 236–246, [[hep-ph/0102098](#)].

- [96] L. Roszkowski, R. Ruiz de Austri, and T. Nihei, *New cosmological and experimental constraints on the CMSSM*, *JHEP* **08** (2001) 024, [[hep-ph/0106334](#)].
- [97] A. B. Lahanas and V. C. Spanos, *Implications of the pseudo-scalar higgs boson in determining the neutralino dark matter*, *Eur. Phys. J.* **C23** (2002) 185–190, [[hep-ph/0106345](#)].
- [98] M. S. Carena *et. al.*, *Reconciling the two-loop diagrammatic and effective field theory computations of the mass of the lightest CP-even higgs boson in the MSSM*, *Nucl. Phys.* **B580** (2000) 29–57, [[hep-ph/0001002](#)].
- [99] S. Abdullin and F. Charles, *Search for SUSY in (leptons +) jets + e(t)(miss) final states*, *Nucl. Phys.* **B547** (1999) 60–80, [[hep-ph/9811402](#)].
- [100] B. C. Allanach, J. P. J. Hetherington, M. A. Parker, and B. R. Webber, *Naturalness reach of the large hadron collider in minimal supergravity*, *JHEP* **08** (2000) 017, [[hep-ph/0005186](#)].
- [101] H. Baer, C. Balazs, A. Belyaev, T. Krupovnickas, and X. Tata, *Updated reach of the CERN LHC and constraints from relic density, $b \rightarrow s$ gamma and $a(\mu)$ in the mSUGRA model*, *JHEP* **06** (2003) 054, [[hep-ph/0304303](#)].
- [102] **CMS** Collaboration, S. Abdullin *et. al.*, *Discovery potential for supersymmetry in CMS*, *J. Phys.* **G28** (2002) 469, [[hep-ph/9806366](#)].
- [103] A. Belyaev, M.-H. Genest, C. Leroy, and R. R. Mehdiev, “Extending LHC reach in the focus point region of supersymmetry.” to appear.
- [104] H. Baer, A. Belyaev, T. Krupovnickas, and X. Tata, *Linear collider capabilities for supersymmetry in dark matter allowed regions of the mSUGRA model*, *JHEP* **02** (2004) 007, [[hep-ph/0311351](#)].
- [105] H. Baer, T. Krupovnickas, and X. Tata, *Two photon background and the reach of a linear collider for supersymmetry in WMAP favored coannihilation regions*, *JHEP* **06** (2004) 061, [[hep-ph/0405058](#)].
- [106] H. Baer, R. Munroe, and X. Tata, *Supersymmetry studies at future linear e^+e^- colliders*, *Phys. Rev.* **D54** (1996) 6735–6755, [[hep-ph/9606325](#)].
- [107] H. Baer, C. Balazs, A. Belyaev, and J. O’Farrill, *Direct detection of dark matter in supersymmetric models*, *JCAP* **0309** (2003) 007, [[hep-ph/0305191](#)].
- [108] J. R. Ellis, K. A. Olive, Y. Santoso, and V. C. Spanos, *Update on the direct detection of supersymmetric dark matter*, *Phys. Rev.* **D71** (2005) 095007, [[hep-ph/0502001](#)].
- [109] **XENON** Collaboration, J. Angle *et. al.*, *First results from the XENON10 dark matter experiment at the Gran Sasso national laboratory*, [arXiv:0706.0039](#).
- [110] **CDMS** Collaboration, D. S. Akerib *et. al.*, *First results from the cryogenic dark matter search in the soudan underground lab*, *Phys. Rev. Lett.* **93** (2004) 211301, [[astro-ph/0405033](#)].
- [111] **The SuperCDMS** Collaboration, R. W. Schnee *et. al.*, *The SuperCDMS experiment*, [astro-ph/0502435](#).
- [112] **Xenon** Collaboration, Y. Suzuki, *Low energy solar neutrino detection by using liquid xenon*, [hep-ph/0008296](#).

- [113] **WARP** Collaboration, R. Brunetti *et. al.*, *WARP liquid argon detector for dark matter survey*, *New Astron. Rev.* **49** (2005) 265–269, [[astro-ph/0405342](#)].
- [114] D. B. Cline *et. al.*, *Status of ZEPLIN II and ZEPLIN IV study*, *Nucl. Phys. Proc. Suppl.* **124** (2003) 229–232.
- [115] J. A. Nikkel, W. H. Lippincott, and D. N. McKinsey, *Neutrino and dark matter detection with CLEAN: Preliminary studies*, *Int. J. Mod. Phys.* **A20** (2005) 3113–3114.